

Cometary x-rays: line emission cross sections for multiply charged solar wind ion charge exchange

S Otranto^{1,2}, R E Olson¹ and P Beiersdorfer^{3,4}

¹ Physics Department, University of Missouri-Rolla, Rolla, MO 65401, USA

² CONICET and Dto. de Física, Universidad Nacional del Sur, 8000 Bahía Blanca, Argentina

³ Department of Physics, Lawrence Livermore National Laboratory, Livermore, CA 94550, USA

⁴ Space Sciences Laboratory, University of California, Berkeley, CA 94720, USA

E-mail: otrantos@umr.edu

Received 12 February 2007, in final form 25 March 2007

Published 30 April 2007

Online at stacks.iop.org/JPhysB/40/1755

Abstract

Absolute line emission cross sections are presented for 1 keV amu⁻¹ charge-exchange collisions of multiply charged solar wind ions with H₂O. These cross sections can be used to model charge-exchange processes with cometary targets with similar binding energies such as H, O, CO₂ and CO. A parameter-free model is used to successfully predict the recently observed x-ray spectra of comet Linear C/1999 S4 and McNaught-Hartley C/1999 T1. We show that the resulting spectrum is extremely sensitive to the time variations of the solar wind composition.

(Some figures in this article are in colour only in the electronic version)

1. Introduction

State-selective single electron capture cross sections for highly stripped multiply charged ions colliding with atoms and molecules are of particular importance not only in basic atomic physics research, but have direct applications to magnetic fusion plasma diagnostics [1–3], to heliospherical and planetary science, [4–6] and to astrophysical observations [7, 8]. In general, such reactions lead to an excited ion which decays via photon emission.

Motivation for the present work is provided by recent observations of x-ray emission from comets as they transit our solar system. In 1996, the Röntgen satellite (ROSAT) focused on the comet P/Hyakutake and observed x-ray emission of unexpected intensity between the comet and the Sun, out to a distance on the order of 10⁶ km from the comet's nucleus [9]. It is now recognized that this emission is due to electron capture between heavy solar wind ions and the gas surrounding the comet [10, 11].

Since solar wind events on the comet and the Earth are subject to a time delay determined by the difference in the speed of light versus that of the solar wind ions, the measurement of

x-ray emission from a comet that is situated inside the orbit of the Earth provides warning of the solar wind ion intensity and composition many hours in advance of these ions' arrival. Hence, the observation of cometary x-ray emission by earth orbiting satellites can be used as solar wind weather stations. It is well known that solar wind bursts can impact computer operation by generating 'phantom commands' from upsets in the memory chips. Other deleterious effects are the impact to astronauts' health and degradation of communication and the global positioning systems. Moreover, since solar wind bursts induce current in long conductors on the ground, they can cause blackouts over major areas, as occurred, for example, in southern Canada and the eastern US in 1989 [12].

To date, astrophysical models for the electron capture reactions have assumed an equal population of the l -values or statistical populations [10, 13, 14]. There is also a model based on Landau–Zener calculations where the l -values are adjusted to reproduce available data [15]. Other analyses have fit the measurements of the Chandra X-ray Observatory (CXO) by means of six to nine emissions, adjusting their positions and intensities [11, 16, 17]. It is clear from these works that there is a strong need of reliable theoretical capture cross sections in order to describe the available data.

Initially, analyses have been based on low-resolution laboratory data available for the reactants and collision energies encountered in comet x-ray emission [18, 19]. However, for hydrogenic projectiles one must be careful to recognize that the $2^3S \rightarrow 1^1S$ transition in the helium-like product ion, which will represent about 50% of the x-ray emission in these systems for comets, is incompletely observed in beam measurements due to their long $\sim 10^{-3}$ s 2^3S lifetime. More recently, laboratory work performed at EBIT with an x-ray micro-calorimeter spectrometer (XRS) provides spectra with an unprecedented ~ 10 eV FWHM resolution [20]. These x-ray spectra are useful as critical benchmarks of theoretical models and include the forbidden triplet transitions for hydrogenic ions due to the long observation time scale of the trap measurements. They have been used to successfully fit the spectrum of Linear C/1999 S4 [20]. However, these data are collected at ~ 0.01 keV amu^{-1} impact energy, while solar wind ion impact energies are 0.8–3.0 keV amu^{-1} . For analysing cometary spectra it is best to rely on data appropriate for higher collision energies, since the line emission changes over such a large energy range [21].

In this work, we combine calculated emission cross sections together with the ion abundances measured by the Advanced Composition Explorer (ACE) to predict cometary spectra. We then show the sensitivity of the spectra that arise from various estimated time delays between the solar wind events at the comet and at the location of the ACE satellite.

For cometary observations, the classical trajectory Monte Carlo (CTMC) model [22] provides a tractable calculational method to study these involved charge-exchange systems. Within the CTMC method, semiclassical methods have been developed to predict the n , l and m_l electron capture excited levels [23] of the projectile and have led over the years to capture and emission cross sections which are in good agreement with experimental data (see, for example, [23, 24]). After electron capture to excited nl levels of the projectile ion, absolute line emission cross sections are determined using a hydrogenic branching and cascading model.

In section 2, the theoretical method is described. In section 3, we use the CTMC method to describe cometary x-ray emission. Two particular cases are chosen for such a task: comets Linear C/1999 S4 and McNaught-Hartley C/1999 T1. The spectra of these two comets were measured under completely differently conditions. The spectrum of the former comet was measured during a very short period of time, while the spectrum of the latter comet was obtained in terms of 1 h snapshots over a one-week period. In this section, we also point out the need of accurate emission cross sections in the astrophysical context, by comparing the present CTMC line emission cross sections with those obtained by means of the models of Wegmann

and Häberli. In section 4, we draw our conclusions and mention possible implications of the present results for future analyses and missions.

2. Theoretical method

In the present treatment we have considered a hydrogenic H₂O target where the binding energies of 12.6 eV and 14.7 eV have been used to represent the 1B1 and 3A1 molecular orbitals. The electron capture data of Richardson *et al* [25] for H⁺ colliding with H₂O indicate that the 1B2 molecular state makes a negligible contribution to the cross section. Thus, we have used branching ratios of 1/2 each for the 1B1 and 3A1 molecular orbitals and 0 for the 1B2. The present approximation considers the problem within a three-body theory and it reasonably predicts the projectile product states.

In the CTMC method, for those events that resulted in charge exchange, a classical number n_c is obtained from the binding energy E_p of the electron relative to the projectile by

$$E_p = -\frac{Z_p^2}{2n_c^2}, \quad (1)$$

where Z_p is the charge of the projectile core. Then, n_c is related to the quantum number n of the final state by the condition

$$[(n-1)(n-1/2)n]^{1/3} \leq n_c < [(n+1)(n+1/2)n]^{1/3}. \quad (2)$$

From the normalized classical angular momentum $l_c = (n/n_c)(\mathbf{r} \times \mathbf{k})$, where \mathbf{r} and \mathbf{k} are the captured electron position and momentum relative to the projectile, we relate l_c to the orbital quantum number l of the final state by

$$l \leq l_c < l+1. \quad (3)$$

The m_l determination is satisfied by

$$\frac{2m_l-1}{2l+1} \leq \frac{l_z}{l_c} < \frac{2m_l+1}{2l+1}, \quad (4)$$

where l_z is the z -projection of the angular momentum obtained from the calculations [23]. The cross section to a definite (n, l, m) state is then given by

$$\sigma_{nlm} = \frac{N(n, l, m)\pi b_{\max}^2}{N_{\text{tot}}}, \quad (5)$$

where $N(n, l, m)$ is the number of events of electron capture to the nlm level and N_{tot} is the total number of trajectories integrated. The impact parameter b_{\max} is the parameter beyond which the probability of electron capture is negligibly small.

In order to obtain emission cross sections $\sigma_{n,l,m \rightarrow n',l',m'}^{(\text{em})}$, cascade contributions from higher $n'' > n$ levels are added and the n, l, m_l populations are multiplied by hydrogenic branching ratios $b_{l \rightarrow l'}$ for the relevant transitions [26] and by their relative line strengths [23]. In this sense, we have assumed the hydrogenic branching ratios to be valid for the high-lying singlet states of the He-like ions.

In table 1, the CTMC line emission cross sections for 1 keV amu⁻¹ solar wind ions colliding with H₂O are presented. These absolute cross sections vary somewhat over solar wind collision energies and are approximately 20% larger at slow solar wind speeds (0.8 keV amu⁻¹) and 20% lower for fast speeds (3 keV amu⁻¹). However, we find that the relative cross sections that are appropriate for comparison to cometary data are insensitive to these energy variations. The H₂O molecule was utilized since it makes up approximately 90% of comet gases [27].

Table 1. Line emission cross sections following single electron capture in 1 keV amu^{-1} collisions of ions with H_2O (10^{-15} cm^2). All the transitions are from the upper level indicated to the ground state. For hydrogenic projectiles the $n\text{p } ^1\text{P}_1$ levels represent the transitions $1\text{snp } ^1\text{P}_1 \rightarrow 1\text{s}^2 ^1\text{S}_0$.

Upper level	C ⁵⁺	C ⁶⁺	N ⁶⁺	N ⁷⁺	O ⁷⁺	O ⁸⁺	Ne ⁹⁺	Ne ¹⁰⁺
1s2s ³ S ₁	1.152	–	1.422	–	1.694	–	2.252	–
1s2p ³ P ₁	0.576	–	0.711	–	0.847	–	1.126	–
2p ¹ P ₁	0.379	1.965	0.491	2.435	0.609	2.985	0.886	4.140
3p ¹ P ₁	0.153	0.353	0.088	0.337	0.084	0.347	0.090	0.360
4p ¹ P ₁	0.044	0.502	0.126	0.450	0.112	0.215	0.033	0.115
5p ¹ P ₁	–	0.023	0.006	0.168	0.042	0.380	0.087	0.182
6p ¹ P ₁	–	–	–	0.004	–	0.021	0.029	0.243
7p ¹ P ₁	–	–	–	–	–	0.001	0.001	0.015
8p ¹ P ₁	–	–	–	–	–	–	–	0.001

The present calculations also provide first-order estimates of the x-ray line emission cross sections for the major comet gases and their photo-dissociated atoms such as CH_4 (12.6 eV), CO_2 (14.4 eV), atomic O (13.6 eV), atomic H (13.6 eV), and CO (14.1 eV) at energies close to 1 keV amu^{-1} (440 km s^{-1}). In a previous publication we have shown that experimental and theoretical cross sections obtained for H_2O , CH_4 and CO_2 at 0.01 keV amu^{-1} were almost identical [21].

To obtain the emission cross sections for the hydrogenic projectiles presented in table 1, we have used those corresponding to a bare projectile with the same charge state. From statistical weight considerations, the singlet spectra were obtained by multiplying the calculated $n\text{p} \rightarrow 1\text{s}$ cross sections by 25%. The remaining x-ray flux then resides in the $n = 2$ triplet states. This is partitioned as 1/3 to the $2^3\text{P} \rightarrow 1^1\text{S}$ transition and 2/3 to the forbidden $2^3\text{S} \rightarrow 1^1\text{S}$ transition. The ratios were derived from the high-resolution measurements of Beiersdorfer on the $\text{Ne}^{9+} + \text{Ne}$ electron capture system [21].

In figure 1, we show the state-selective capture cross sections for the different projectiles here considered at an impact energy of 1 keV amu^{-1} . It can be seen that as the projectile charge increases, so does the n_{max} -value where the distribution peaks in agreement with the $q^{3/4}$ scaling. In contrast to the low energy case, where the captured electrons mainly populate the $l = 1$ states, at these keV amu^{-1} energies higher l -values within a given n -level are preferentially populated. On the other hand, it is also clear that the statistical limit has not been reached at the present impact energy.

Absolute line emission cross sections following collisions of He^{2+} with CH_4 , H_2O , CO_2 and CO have been recently published for several collision energies [28]. In figure 2, we present the available data together with the present predictions for H_2O . The low projectile charge considered leads to most of the emission being concentrated in the Lyman- α line, with the other Lyman lines contributing less than 10% to the total emission. It can be seen that the CTMC method provides a good description the dominant electron capture to the $n = 2$ level along with the branching to the 2p state that determines, along with contributions from cascades, the Lyman-alpha line emission absolute magnitude. We find that the present results for H_2O slightly underestimate the Lyman- β line. No data are available to check our predictions for the Lyman- γ transition. It is also worth noting how similar the emission cross sections of the different targets are. This reinforces our previous statement that the present cross sections can be used to describe line emission cross sections from targets with similar ionization potentials.

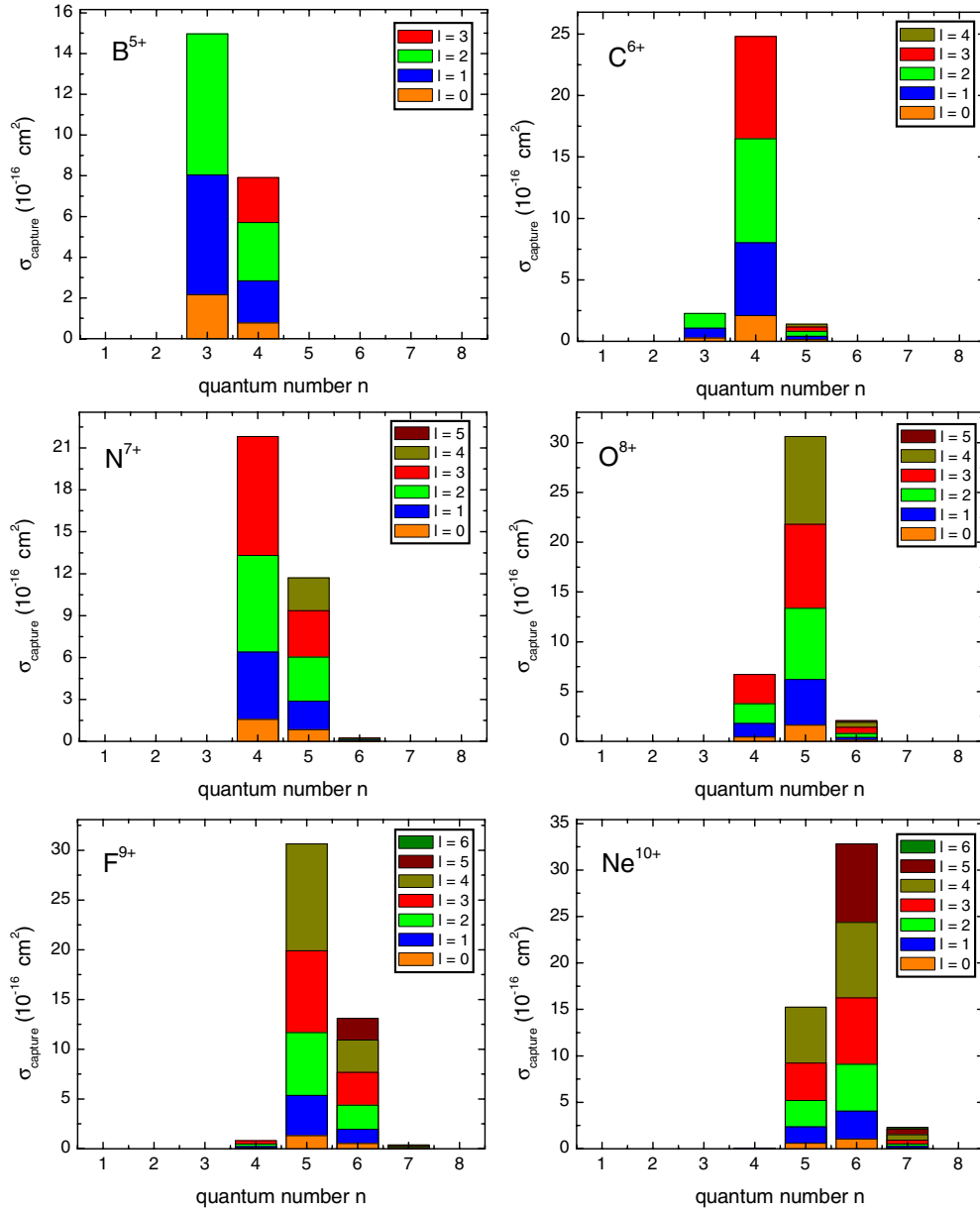


Figure 1. CTMC state-selective single electron capture cross sections for collisions involving bare projectiles ($q = 5, \dots, 10$) and H_2O target.

3. Applications to cometary x-ray emission

From the tabulated cross sections of table 1, the charge-exchange-produced x-ray emission for cometary spectra can be constructed. In order to compare to the Chandra X-ray Observatory (CXO) data, the emission lines were multiplied by the ACIS-S spectrometer effective area and then convoluted with a 100 eV FWHM Gaussian function [17]. The lines corresponding to

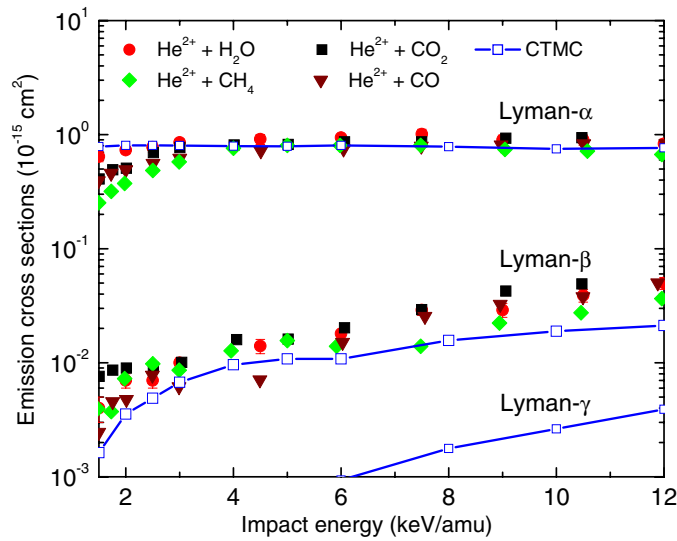


Figure 2. Line emission cross sections for He^{2+} colliding on several cometary targets as a function of the impact energy. The experimental data are those of [28].

each solar wind ion are weighted by the corresponding abundance in the solar wind appropriate for the time during which the x-ray measurements took place.

The solar wind ion abundances are available in 2 h intervals in terms of $[\text{C}/\text{O}]$, $[\text{C}^{q+}/\text{C}]$ and $[\text{O}^{q+}/\text{O}]$ ratios [29] and are based on ACE/SWICS-SWIMS (the latter for Solar Wind Ion Mass Spectrometer) satellite measurements. The accuracy of the ion observations is estimated to be 10–15% [29]. The ACE is an L1 orbiting satellite and the time delay of the solar wind events on the satellite compared to the Earth is of about 1 h. In the present analysis we consider ACE measurements as if they were based on the Earth.

3.1. Linear C/1999 S4

In figure 3, we show the ion abundances for the C^{5+} , C^{6+} , O^{7+} and O^{8+} ions appropriate for the period (from 4:30 to 8:04 UT) in which the spectrum of comet Linear C/1999 S4 was measured by the CXO on 14 July 2000. The figure also clearly illustrates the large variations in ion composition as a function of the hour of the day.

A critical point when the measured ion abundances are used to describe cometary spectra is the difference in time between the solar wind events at the Earth-orbiting satellite measuring the ion abundances and those at the comet coma. In the following, we have used the full solar wind delay estimation of +0.7 days [11]. To illustrate the sensitivity of the spectrum to time variations, we display how it would appear if the solar wind conditions were shifted by ± 1 days.

In figure 4, we present calculated x-ray spectra for Linear C/1999 S4 considering a collisionally thin target with the solar wind delays given above. For x-ray emission energies between 200 eV and 300 eV, we have included lines of $\text{Mg}^{8+,9+}$ and Si^{8+} . Here, we have used the CTMC intensities of the Balmer transitions corresponding to a bare projectile with charge equal to that of the projectile. After averaging the solar wind abundances provided by Schwadron and Cravens [30], the Mg^{9+} and Si^{9+} projectiles have been assumed to have equal abundances, about 20% less than that of Mg^{10+} . In the present case, a Mg^{10+} abundance

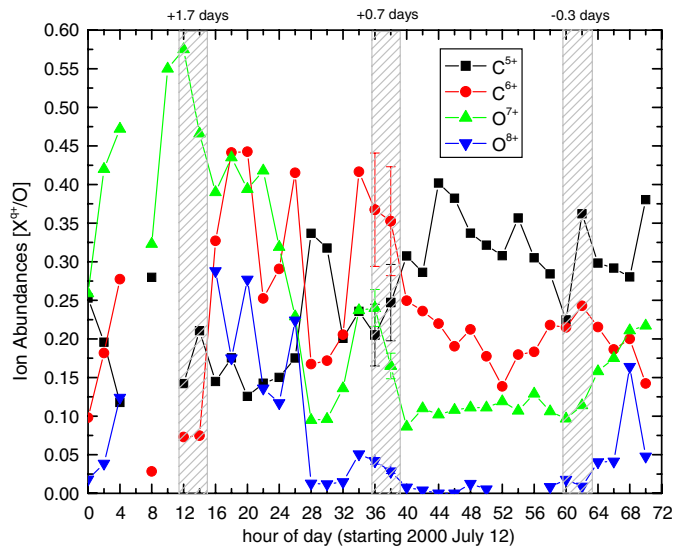


Figure 3. Solar wind ion abundances as a function of time during the measurement of the spectrum of Linear C/1999 S4 measured by ACE.

of 0.38 was used. Whether our treatment of these lines is appropriate is not clear due to the rapidly decreasing sensitivity of the spectrometer in this region. However, such a background must be included since their lines overlap those of the C ions because of the 100 eV CXO resolution. The lines corresponding to N^{6+} and N^{7+} were weighted by the solar wind abundance provided by Schwadron and Cravens [30].

In figure 4(a), we compare the spectra obtained when considering the $C^{5+,6+}$ and $O^{7+,8+}$ abundances corresponding to the appropriate delay (measured on 13 July) with those obtained for the ion abundances found one day before and one day after the spectral measurement. The spectra have been normalized to the O^{7+} line located at approximately 560 eV. As it can be seen, the time variation of the carbon to oxygen ion abundances gives rise to major changes in the spectra. We find that the spectra are not only sensitive to the overall intensity of the solar wind flux, but also to the hour-by-hour changes in the relative abundances of the solar wind ions.

In figure 4(b), we display the spectral lines with 10 eV FWHM resolution, as might be realized in future XRS observations. A rich spectrum is obtained that will test our atomic physics knowledge. It is readily apparent that the high-lying $np \rightarrow 1s$ transitions are very important and must be correctly portrayed in cometary models. Furthermore, the spin forbidden $2^3S \rightarrow 1^1S$ and $2^3P \rightarrow 1^1S$ splitting is readily observed after capture by O^{7+} ions.

3.2. McNaught-Hartley C/1999 T1

Comet McNaught-Hartley was observed at the beginning of January 2001, near the period of its maximum brightness. The observing conditions have been presented by Krasnopolsky *et al* [16].

In figure 5, we show the ion abundances for the C^{5+} , C^{6+} , O^{7+} and O^{8+} measured at the beginning of January 2001. The small boxes show the nearly 1 h snapshots during which the CXO measurements took place. In the following we use a time delay of +6.12 days, close

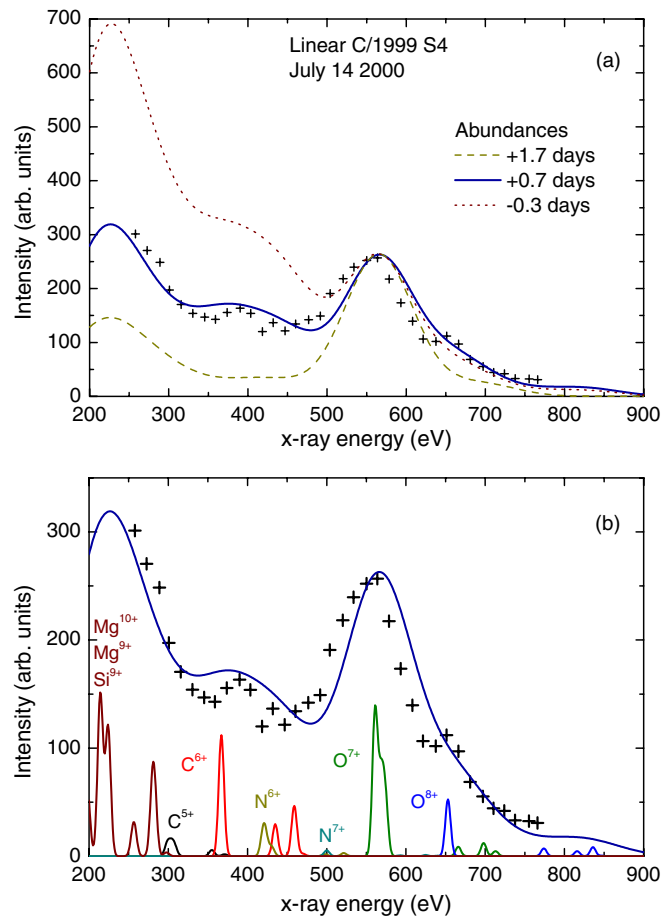


Figure 4. (a) Calculated x-ray spectra for Linear C/1999 S4 with FWHM of 100 eV. The full delay of solar wind events (+0.7 days) is compared with the predictions obtained with ion abundances from one day before and one day after the observation; (b) the calculated x-ray spectra are shown with FWHM of 100 eV and 10 eV to simulate the CXO ACIS-S and the XRS resolutions.

to that of 6 days estimated by the Krasnopolsky *et al* [16]. We have used the mean x-ray luminosities to weight the contribution of each snapshot to the resulting spectrum.

In figure 6, we present the results obtained for the different snapshots as well as the final result. The lines corresponding to N^{6+} and N^{7+} were weighted by the slow solar wind abundance provided by Schwadron and Cravens [30] and for the Mg^{10+} an abundance of 0.25 was used in order to correct the low energy part of the spectrum. From figures 5 and 6, it can be seen that the O^{8+} abundance was high during 2 January 2001 (it doubles the slow solar wind value of 0.07 tabulated by Schwadron and Cravens based on averages of Ulysses data [30]). This left a clear trace in the resulting spectrum, even though its contribution was much less important between the second and fifth snapshots.

3.3. The need of accurate emission cross sections in the astrophysical context

In the following, we illustrate the need for atomic physics data that provides accurate l -states population after the charge-exchange process. As we have already pointed out above,

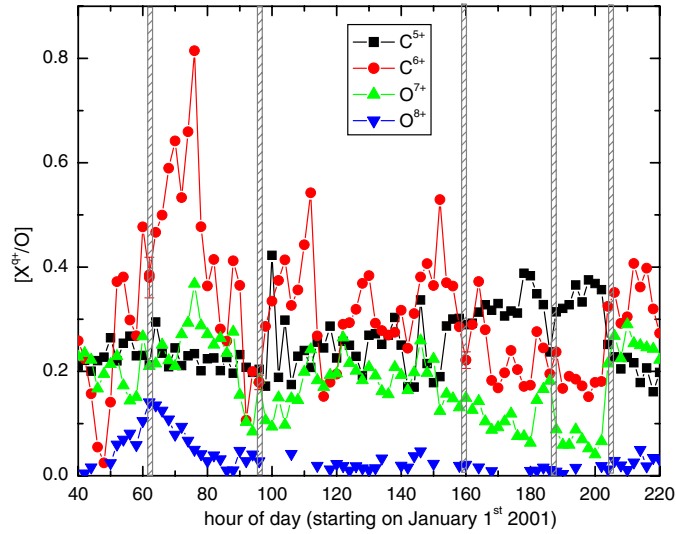


Figure 5. Solar wind ion abundances as a function of time during the measurement of the spectrum of McNaught-Hartley C/1999 T1 measured by ACE.

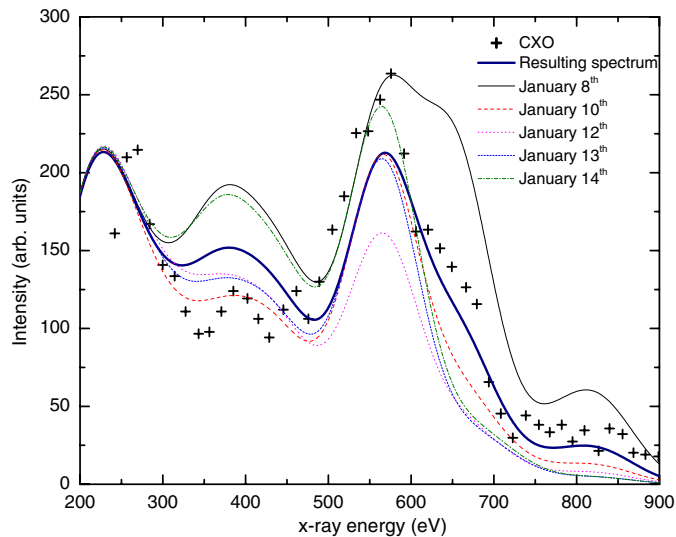


Figure 6. Calculated x-ray spectra for McNaught-Hartley C/1999 T1 with FWHM of 100 eV. The spectrum for each snapshot is presented together with the resulting spectrum

previous treatments have been either based on the assumption of the high-energy statistical limit in which all the emission can be assumed to be due to the $n = 2 \rightarrow n = 1$ transition [14] or equally probable emissions from $n = 2, \dots, n_{\max}$ to the ground state [13]. While the former assumption clearly underestimates the higher Lyman lines, the latter tends to overestimate the higher Lyman lines and does not show any kind of energy dependence for the Lyman lines. It was shown by Beiersdorfer *et al* in 2001 that these two models fail to predict the shape of the emission cross sections following Ne^{10+} and Ne^{9+} collisions on Ne, when compared to

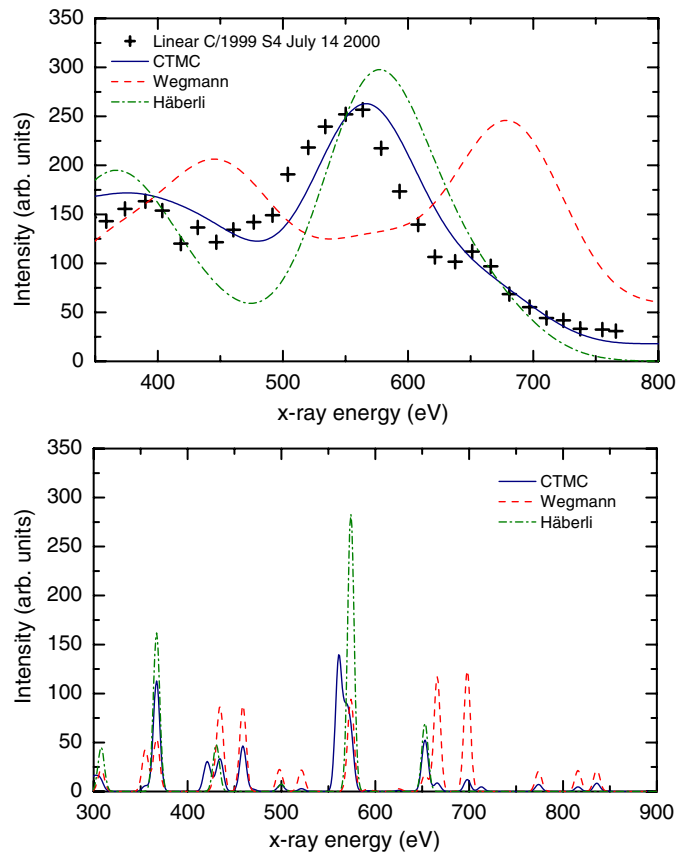


Figure 7. (a) Theoretical spectrum for Linear C/1999 S4 with FWHM of 100 eV according to the CTMC method and the Wegmann and Häberli models. The ion abundances used are the same as in figure 3. (b) The same spectrum as in (a) but for 10 eV resolution.

data obtained with EBIT-II [31]. Note that the predictions of the CTMC method are in good agreement with the data for both systems [21].

One of the advantages of the CTMC method is that it inherently provides the population of the l -levels for each n -level, which is vital in order to obtain the corresponding emission cross sections. In order to show this, in figure 7 we compare the Linear C/1999 S4 spectrum calculated with the CTMC method and by using Häberli and Wegmann models. In figure 7(a), the 100 eV resolution CXO spectrum is compared to the theoretical results while in figure 7(b) the theories are shown with 10 eV resolution. It can be seen that the overestimation of the higher Lyman lines by the Wegmann model leads to two peaks located at about 450 eV and 690 eV which are in total disagreement with the data. The Häberli model, on the other hand, even though providing closer agreement to the measured spectrum, clearly underestimates the higher Lyman lines of the C^{6+} projectile and underestimates the data in the 400–550 eV region. In addition, the low energy peak around 400 eV is clearly shifted to lower energies.

In this sense, the CTMC model provides a much more accurate description of the spectrum. It seems clear that if in years to come cometary x-rays are measured with high-resolution microcalorimeter spectrometers (like that used by Beiersdorfer *et al* [20] to obtain high-resolution laboratory x-ray spectra following charge exchange between typical solar wind

ions and cometary targets) theoreticians will face a big challenge to accurately describe the spectra.

4. Conclusions

To summarize, we have presented CTMC calculated emission cross sections for several projectiles following charge exchange with H₂O target. In the present scheme, its 1B1 and 3A1 molecular orbitals have been explicitly considered. The tabulated cross sections have been used to provide a theoretical spectrum of comets Linear C/1999 S4 and McNaught-Hartley C/1999 T1 by using ACE data for the ion abundances. Quantitative agreement has been obtained with the CXO data. Furthermore, the underlying CXO spectra has been presented for Linear C/1999 S4 with a 10 eV FWHM convolution to mimic a micro-calorimeter spectrometer such as the one launched on the Suzaku satellite in 2005. Unfortunately, after launch the spectrometer's cryogenics failed three weeks into the mission. These high-resolution spectra clearly show the details of the charge-exchange processes and resolve forbidden transitions for hydrogenic projectiles.

For McNaught-Hartley C/1999 T1, we have taken into account the fact that the resulting spectrum was measured in five 1 h snapshots during a one-week period. We have discussed how the relative contribution of the individual snapshots contributed to shape the final spectrum. We have shown that here the presented cross sections provide much better agreement with the data than previous approximations that were based on high-energy limits or a not so accurate distribution of the emission intensity in the main Lyman lines.

We emphasize that the x-ray spectrum requires solar wind ion abundances measured on the same time scale as the x-ray observations. Based on the present results we conclude that in order to perform proper analyses on the solar wind ion abundances, future missions should be conceived to measure x-ray spectra continuously during a short period of time instead of taking snapshots over several days. Furthermore, cases in which the solar wind ions hit the comet first and then the Earth can be used to provide timely information about the solar wind ion composition on the Earth several hours in advance. This would be of great importance in order to avoid or prevent space-weather-related failures on satellites, communications and navigational systems.

Acknowledgments

This work has been supported by the Office of Fusion Energy Sciences, DOE. Work in LLNL performed under the DOE contract W-7405-ENG-48 and NASA's Planetary Atmospheres Program grant NNG06GB11G. Work in UNS supported by PGI 24/F038 and PICTR03/00437 of ANPCyT.

References

- [1] Källne E, Källne J, Dalgarno A, Marmar E S, Rice J E and Pradhan A K 1984 *Phys. Rev. Lett.* **52** 2245
- [2] Rice J E, Marmar E S, Terry J L, Källne E and Källne J 1986 *Phys. Rev. Lett.* **56** 50
- [3] Beiersdorfer P, Bitter M, Marion M and Olson R E 2005 *Phys. Rev. A* **72** 032725
- [4] Cravens T E 2000 *Astrophys. J. (Lett.)* **532** L153
- [5] Dennerl K 2003 *Astron. Astrophys.* **394** 1119
- [6] Dennerl K 2006 *Astron. Astrophys.* **451** 709
- [7] Wargelin B J and Drake J J 2001 *Astrophys. J. (Lett.)* **546** L57
- [8] Tanaka Y 2002 *Astron. Astrophys.* **382** 1052
- [9] Lisse C M *et al* 1996 *Science* **274** 205

- [10] Cravens T E 1997 *Geophys. Res. Lett.* **24** 105
- [11] Lisse C M *et al* 2001 *Science* **292** 1343
- [12] 1997 Space Weather: A Research Perspective *National Academy of Sciences Report*
- [13] Wegmann R *et al* 1998 *Planet. Space Sci.* **46** 603
- [14] Häberli R M *et al* 1997 *Science* **276** 939
- [15] Rigazzio M, Kharchenko V and Dalgarno A 2002 *Phys. Rev. A* **66** 064701
- [16] Krasnopolsky V A *et al* 2002 *Icarus* **160** 437
- [17] Krasnopolsky V A 2004 *Icarus* **167** 417
- [18] Greenwood J B *et al* 2000 *Astrophys. J.* **533** L175
- [19] Greenwood J B *et al* 2001 *Phys. Rev. A* **63** 062707
- [20] Beiersdorfer P *et al* 2003 *Science* **300** 1558
- [21] Otranto S, Olson R E and Beiersdorfer P 2006 *Phys. Rev. A* **73** 022723
- [22] Olson R E and Salop A 1977 *Phys. Rev. A* **16** 531
- [23] Schippers S *et al* 1995 *J. Phys. B: At. Mol. Opt. Phys.* **28** 3271
- [24] Knoop S *et al* 2005 *J. Phys. B: At. Mol. Opt. Phys.* **38** 1987
- [25] Richardson P G *et al* 1986 *J. Chem. Phys.* **84** 3189
- [26] Bethe H A and Salpeter E E 1957 *Quantum Mechanics of One- and Two-Electron Atoms* (Berlin: Springer)
- [27] Biver N *et al* 2002 *Earth Moon and Planets* **90** 323
- [28] Bodewitz D, Hoekstra R, Seredyuk B, McCullough R W, Jones G H and Tielens A G G M 2006 *Astrophys. J.* **642** 593
- [29] Raines J, Lepri S and Zurbuchen T http://www.srl.caltech.edu/ACE/ASC/level2/lvl2DATA_SWICS.html
- [30] Schwadron N A and Cravens T E 2000 *Appl. Phys. J.* **544** 558
- [31] Beiersdorfer P, Lisse C M, Olson R E, Brown G V and Chen H 2001 *Astrophys. J. Lett.* **549** L147